PERGAMON

Electrochimica Acta 46 (2001) 2353–2361

ELECTROCHIMICA Acta

www.elsevier.nl/locate/electacta

Use of wavelets to study electrochemical noise transients

A. Aballe, M. Bethencourt, F.J. Botana *, M. Marcos, J.M. Sánchez-Amaya

Universidad de Cádiz, Departamento de Ciencia de los Materiales, Avda. República Saharaui s/n, CASEM, 11510 Puerto Real, Cádiz, Spain

Received 7 August 2000; received in revised form 4 December 2000

Abstract

Two kinds of time records are found when measuring electrochemical noise: those presenting characteristic transients or spikes, and others in which neither transients nor spikes can be distinguished. Although the former are likely to be more informative than the latter, most of the methods developed for analyzing electrochemical noise are focused on studying the latter. This paper suggests a methodology for automatically studying the appearance of the transient, which could represent a significant advance in the field of corrosion monitoring and laboratory investigation. The proposed methodology is based on a mathematical tool called the wavelet transform, whose principal characteristic is that it enables a simultaneous analysis of signals in both time and scale. Thus a subsequent interscalar analysis of the signals can reveal the existence of transients and even provide a comparative characterization of their size and scale.

Keywords: Electrochemical noise; Wavelet analysis; Transient detection; Corrosion; Monitoring

1. Introduction

The interpretation of data from electrochemical noise measurements (ENM) frequently requires using detailed analysis. The most appropriate method depends on the features of the particular electrochemical noise (EN) signal. We can distinguish two main kinds of EN time records: those in which it is possible to recognize distinctive-shaped spikes and those formed by irregular fluctuations. EN time records containing transients are generally considered to contain more information than the other kind. In fact, recently, various experimental arrangements have been proposed to encourage the appearance of transients [1–3]. Generally, the analysis of spikes is achieved by visual inspection, which complicates the monitoring of the signal. Nowadays, there are commercial software applications that are able to detect transients. However, they are usually not very efficient since the spike detection is based simply on establishing a threshold value over the raw data.

The most commonly-used EN analysis methods (statistical and spectral) were devised for stationary signals that do not show distinctive transients [4]. The main disadvantage of those methods is that they analyze signals by averaging the features across the whole time record. To avoid this limitation, the discrete wavelet transform (DWT) has been proposed [5,6] for the study of both stationary and non-stationary EN time records. In the cited papers, the use of a new kind of representation, energy distribution plots (EDPs), is proposed to discriminate different types of EN records when power spectral density plots fail. In addition, the development of two corrosion processes that evolve simultaneously in the same system has been monitored separately by using wavelet transform [7].

The discrete wavelet transform consists in expressing a discrete signal, x_n $n = 1, 2, \ldots, N$, as a function of a series of basis function $\phi_{j,n}$ and $\psi_{j,n}$ [8]:

* Corresponding author. Tel.: +34-956-830828; fax: +34-956-016040.

E-mail address: javier.botana@uca.es (F.J. Botana).

0013-4686/01/$ - see front matter
PII: S0013-4686(01)00424-8

$$x_n \approx \sum_n s_{J,n}\phi_{J,n} + \sum_n d_{J,n}\psi_{J,n} + \sum_n d_{J-1,n}\psi_{J-1,n} + \cdots + \sum_n d_{1,n}\psi_{1,n} \quad (1)$$

where $s_{J,n}$, $d_{J,n}$, $d_{J-1,n}$, $d_{1,n}$ are vectors termed 'crystals' which contain wavelet coefficients. The term 'crystal' is used because the wavelet coefficients in a crystal correspond to a set of translated wavelet functions arranged in a regular lattice [8]. The wavelet coefficients in $s_{J,n}$ are also called smooth coefficients, while the remaining wavelet coefficients in Eq. (1) are called detail coefficients. Each crystal describes the original signal on a different scale. The scale of the crystals is given by the subscript j while J is the maximum scale analyzed. The basis functions $\phi_{j,n}$ and $\psi_{j,n}$ are generated by scaling and translating the so-called father wavelets ϕ and mother wavelets ψ, which constitute a pair of oscillating functions with a limited span of time.

The aim of this study is to devise an automatic method based on wavelet analysis for the study of study time records containing transients. Specifically, we propose an algorithm which can enable the position of the transients to be located and the transients to be classified in terms of their time constant and size. A discussion in greater depth of the use of wavelets to analyze electrochemical noise can been found in Ref. [5].

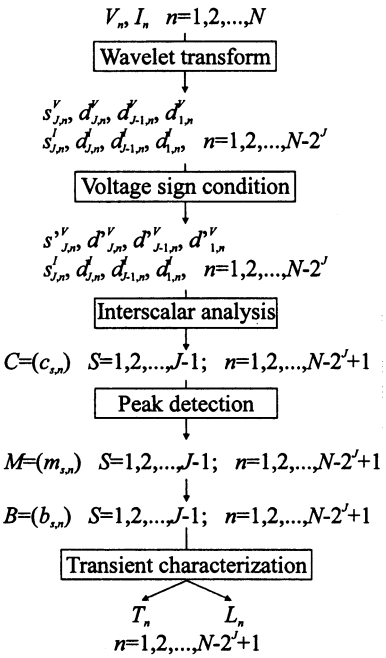

Fig. 1. Diagram of the steps in the proposed algorithm.

2. Transient-detecting algorithm

As mentioned above, the use of the wavelet transform to detect and classify transients in EN time records is proposed in this paper. The position of the transient will be provided by indicating the beginning of the transient, while the classification will consist of two parameters: the scale of the transient and its size. Furthermore, it will be assumed that transients can overlap one another, therefore a 'transient' with several peaks will be considered as several transients. To achieve this, an algorithm based on DWT is proposed here. This algorithm can be divided into five steps, Fig. 1, each of which is explained in detail below.

2.1. Non-decimated wavelet transform

The first step in the algorithm is to decompose the voltage and current signals using a non-decimated wavelet transform, also known as the stationary wavelet transform or translation invariant wavelet transform [8]. This transformation is a variation of the orthogonal discrete wavelet transform used in [5]. Unlike the classical DWT, which has fewer coefficients at coarser scales, each crystal for the non-decimated DWT has N coefficients where N is the number of points in the signal data set [8]. Thus, there is a wavelet coefficient in each crystal associated with every data point. This characteristic makes it possible to perform an interscalar analysis, which is the basis of step 3 in this algorithm.

An important parameter to be selected when it comes to performing a wavelet transform is the pair of wavelets, ϕ and ψ, used to compute the coefficients. In order to perform the transient detection proposed in this paper, the mother wavelet should be as close as possible in appearance to the transients, while the father wavelet is determined by the choice of mother wavelet. However, mother wavelets are functions that oscillate around zero for a number of times, while transients in EN are usually represented by a deviation from and subsequent return to the mean (but which does not repeatedly cross the stable mean value). Therefore, it is difficult to find a mother wavelet that fits the transient shape. Nevertheless, we have found that the so-called Haar wavelets yield a fairly good result, since their shape provides an emphasis of the sudden change that a transient causes in the signal. Furthermore, the simplicity of this kind of wavelet makes it easier to implement the algorithm in a monitoring system.

As pointed out in Ref. [5], one of the advantages of classical DWT against FFT is that it is possible to apply a variety of boundary conditions that avoid undesired effects. In the case of non-decimated DWT, these boundary conditions are limited to extending the signal as if it were periodic, as in the case of FFT.

Therefore, every coefficient calculated through a wavelet basis that exceeds the time record limits is influenced by the boundary effect. Nonetheless, due to the localized nature of the wavelet basis functions (the oscillations damp down to zero quickly), only a few coefficients at the boundaries of the crystals are influenced by this effect. Thus, the problem is solved in this algorithm by ruling out the points associated with those coefficients. Since the width of the wavelets used to deduce each crystal increases with the crystal number j, the number of coefficients to be discounted in each crystal depends on j. So, the first $2^{j-1}-1$ and the last 2^{j-1} wavelet coefficients must be removed from every crystal. Thus, if J is the highest crystal used in the wavelet transform, the data points to be utilized in the analysis are those that occupy the 2^{J-1} to the N-2^{J-1} positions. To sum up, from a signal x_n $n=1, 2, \ldots, N$, this step provides $J+1$ crystals:

$s_{J,n}$, $d_{J,n}$, $d_{J-1,n}$, $d_{1,n}$

each of which describes x_n $n=2^{J-1}, \ldots, N-2^{J-1}$ at different scales by means of $N-2^J+1$ wavelet coefficients. Therefore, when this procedure is applied to the current and voltage noise signal, the following crystals are yielded:

$s^V_{J,n}$, $d^V_{J,n}$, $d^V_{J-1,n}$, …, $d^V_{1,n}$ and

$s^I_{J,n}$, $d^I_{J,n}$, $d^I_{J-1,n}$, …, $d^I_{1,n}$

where the superscripts I and V refer to the origin of the crystals — either current noise or voltage noise. However, the smooth wavelet coefficients, $s_{J,n}$ will not be used any more in this algorithm as they provide a description of the signal at a very large scale, which is of no interest for the study of transients.

2.2. Voltage sign condition

Transients usually appear in EN time records when the electrodes are undergoing a localized corrosion process. In such cases, positive and negative current transients arise randomly in the same time record, depending on the electrode in which the anodic process occurred at the time. However, the corresponding voltage transients have the same sign. So, for example, a micropit initiation often involves a sudden voltage decrease followed by voltage recovery as consequence of the subsequent cathodic reaction [9].

Owing to the shape of the Haar wavelet, a signal decrease on a given scale gives rise to a positive wavelet coefficient and vice versa. We take advantage of this characteristic to construct the first rejection criteria for discarding those data points not corresponding to the beginning of a transient. Thus, this step consists of creating a new series of vectors, $d'^V_{J,n}$, $d'^V_{J-1,n}$, …, $d'^V_{1,n}$, from the J voltage detail crystals obtained in the previous step, so that all negative coefficients are reduced to zero, when negative voltage excursions are expected. Otherwise, the coefficients that are reduced to zero are the positive ones. The time positions of all the zero coefficients are ruled out by this procedure.

2.3. Interscalar analysis

An interscalar analysis consists of studying the correlations among wavelet coefficients of different crystals for each instant. This type of analysis has previously been used in the phase identification in seismograms [10]. The main idea behind this step is that the most pronounced features of the EN signals should appear in the wavelet coefficients across several crystals. Thus, the principal criterion for deciding whether or not a transient begins at a given time is that there must be a high correlation across several scales.

A time function that measures the correlation among some crystals, a correlation function, can be constructed by multiplying the corresponding crystals so as to obtain another vector with the same number of elements as the crystals. Thus, when every crystal has a high coefficient at a given position, the correlation function will show an unusually high value at such a position. So, the third step in this algorithm consists of constructing the correlation functions needed to find the transients. This is the key step of the algorithm because these correlation functions will define what we consider to be a transient. The general expression suggested here for the correlation function is based on three principles:

1. the time constant of the transient can vary. Consequently, it is necessary to define several correlation functions, each of which would detect transients with different time constants. These correlation functions will be grouped as rows in a matrix.
2. a transient entails a change in both the current and voltage signals. Therefore, the correlation function must include crystals from both voltage and current signals.
3. the shape of the transient is that of a sudden beginning followed by a slower decay. Transients with a high time scale (or time constant) will contain components from lower scales also. This means that each correlation function must include crystals from a given scale and the remaining crystals corresponding to lower scales.

In accordance with these principles, the following matrix of correlation has been defined:

$$C=(c_{S,n})=\left(\left|\prod_{1}^{j=S+1} d^I_{j,n-1+2^{J-1}}\cdot d'^V_{j,n-1+2^{J-1}}\right|\right)$$

$$S=1, 2, \ldots, J-1;\ n=1, 2, \ldots, N-2^J+1 \qquad (2)$$

whose rows are correlation functions for the different scales, S. Notice that the absolute value has been taken

in Eq. (2) because the sign of the wavelet coefficient only indicates in which working electrode the anodic process occurred. However, this operation could be omitted when analyzing the asymmetry of the pair of working electrodes.

2.4. Peak detection

The rows of C ($c_{S,n}$ for a given S) are vectors that show a series of outstanding peaks, indicating the presence of transients at the scale determined by S. The aim of this step is to locate those peaks. For this purpose, a new matrix, $M=(m_{S,n})$, is constructed from C by reducing to zero the elements of C that are not maxima, i.e. those points of C whose value is not higher than the value of the preceding and following points in its row:

$$\begin{array}{ll} m_{S,n}=c_{S,n} & \text{if} \quad c_{S,n-1}<c_{S,n} \text{ and } \quad c_{S,n}>c_{S,n+1} \\ m_{S,n}=0 & \text{otherwise} \end{array}$$

where $S=1, 2, \ldots, J-1$; $n=1, 2, \ldots, N-2^J+1$

$$\begin{array}{ll} m_{S,1}=c_{S,1} & \text{if} \quad c_{S,1}>c_{S,2} \\ m_{S,1}=0 & \text{otherwise} \end{array} \tag{3}$$

$$\begin{array}{ll} m_{S,N-2^J+1}=c_{S,N-2^J+1} & \text{if} \quad c_{S,N-2^J}<c_{S,N-2^J+1} \\ m_{S,N-2^J+1}=0 & \text{otherwise} \end{array}$$

The distribution function of each row of M is considered to define which maxima stand out. These distribution functions reveal the outstanding peaks by isolating them from other maxima all with very similar values. In other words, a gap is established between the majority of the peaks and a few of them. Thus, a vector, λ_S, containing the upper limit of the gap for each row is established. All the elements in each row of M with values higher than the corresponding element in λ_S are considered to correspond to transients.

To locate the gap, the rows of M are ranked with their elements in ascending order. We then consider that the gap appears when the subtraction of two consecutive elements of those rows in order gives a value higher than a threshold, δ. This threshold can be defined as a function of the studied signal by determining it as the subtraction of the maximum from the minimum (with exception of the zero value) of each row of M divided by X, where X must be provided by the user's experience. However, the value of X is not decisive because the gap is usually very broad and a large range of X values is suitable.

Once this step has been performed, the positions of the transients for each S value are reflected by creating a new matrix termed $B=(b_{S,n})$ so that:

$$\begin{array}{ll} b_{S,n}=0 & \text{if} \quad m_{S,n}\le\lambda_S \\ b_{S,n}=d^I_{S+1,n-1+2^J-1} & \text{if} \quad m_{S,n}>\lambda_S \end{array} \tag{4}$$

where $S=1, 2, \ldots, J-1$; $n=1, 2, \ldots, N-2^J+1$. Notice that although the criteria for detecting the existence of a transient takes into account both voltage and current signals, the matrix B is composed of either 0 or current wavelet coefficients. Therefore, the subsequent characterization of these transients (the next step) will be performed for current transients.

For any given time (a column of B), there can be three possible results:

1. none of the transients begin in this position ($b_{S,n}=0$ in the entire column of B)
2. there is a transient only for one value of S ($b_{S,n}\neq 0$ for only one element of the B column)
3. a transient is detected for various S values ($b_{S,n}\neq 0$ for more than one element of the B column).

Thus, a transient is considered to occur for every position that follows cases (2) or (3). However, the cases (2) or (3) are quite often detected in two adjacent positions, n and $n+1$. Nonetheless, we have found that both columns of B refer to the same transients, which is not sudden enough to be reflected in one single position. Therefore, on such occasions, the non-zero elements of B in the column $n+1$ are considered to be in the column n.

2.5. Transient characterization

The purpose of this final step is to characterize the transients according to their size and scale. The transients can be classified in respect of size by using the vector L_n defined as follows:

$$L_n=\sum_{S=1}^{J-1} b_{s,n} \tag{5}$$

So, for a given n, $L_n=0$ if none of the transients start at this moment. Under different conditions, L_n yields a transient size evaluation, so that a higher L_n means a higher transient.

In addition, the transients can be characterized according to their scale by taking into account the S values in which a transient is detected. The following vector can be created to characterize the scale of the transients:

$$T_n=\frac{\sum_{S=1}^{J-1} b_{s,n}S}{\sum_{S=1}^{J-1} b_{s,n}} \tag{6}$$

Again, if $T_n=0$ for a given n, it means that none of the transients begin in such a position. Otherwise, T_n provides a comparative estimate of the transient scale, so that the higher T_n, the higher the scale. Notice that the definition of T_n is a weighted average of the S values where the transient is detected.

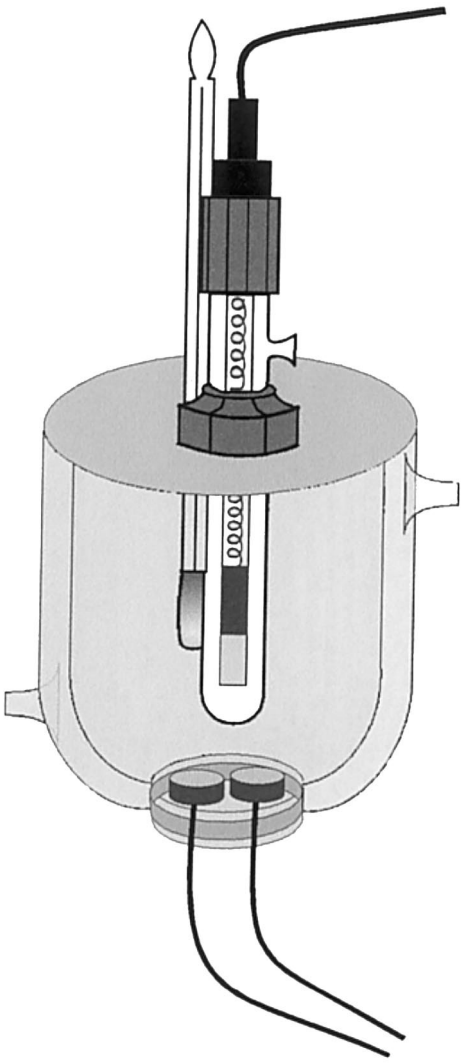

Fig. 2. Measurement cell.

3. Experimental

In order to show the ability of the proposed algorithm to deal with transients, time records containing transients with different characteristics (numbers of transients, arrival distributions, transient shapes, etc) have been considered. All the systems studied have in common that the working electrodes (WEs) are made of type AA5083 aluminium alloy and the medium is a 0.6 M NaCl solution. Nevertheless, modifications to the medium and to the cell configuration, together with changes in the exposure time or sample finish, are made in order to produce differences in the characteristics of the time records under study. However, the origin of the time records is not important because they are used only as realistic examples for the purposes of this paper, not for studying the corrosion implications.

In general, cylindrical samples were cut from a plate of AA5083 Al–Mg alloy, which were coated and mounted in epoxy resin so that only one flat face with an area of 1 cm^2 was exposed to the solution and there was a layer on the edge of the electrode to prevent crevice corrosion from occurring. Prior to the corrosion tests, the metal samples were wet-abraded down to 1200 grade SiC finish, then rinsed with distilled water. In addition, an electrical connection was provided on the back of each electrode to enable electrochemical measurements. Since ENM needs two working electrodes, two samples were mounted very closely in the same epoxy block. Thus, a cell will be constituted by such a block in a solution tank together with a saturated Ag/AgCl reference electrode placed above the specimen, Fig. 2.

ENM records, containing 2048 data points, were collected at 2.15 points per second. Both potential and current noise signals were measured simultaneously, at open circuit potential, using a 1287SI electrochemical interface controlled by CorrWare software. A specific data analysis routine was developed, using the S+ Wavelets toolkit of the S-PLUS software, to develop the algorithm presented here. The calculations performed in a current PC take only few minutes; therefore the algorithm can be used for monitoring applications.

4. Results and discussion

In this section different experimental signals will be analyzed using the algorithm described above. However, it is necessary first to fix those parameters not determined in the algorithm. Thus in order to establish the threshold defined in section 2.4, a value of 100 will be used for X, since we have found that this represents an efficient threshold for a variety of cases. A better result would have been obtained if we had adjusted the user's parameter for each time record. But this has not been done because we have preferred to show that the same algorithm can work quite well for different types of time records. However, it could be interesting to find a more suitable user's parameter for some applications.

The number of crystals used, J, together with the sampling interval Δt, determines the scale range studied ($2\Delta t$, $2^J\Delta t$). In addition, it should be noticed that the number of data points N and the wavelets used limit the maximum value for J that can be chosen. Using the Haar wavelet with $N = 2048$, it is possible to compute up to $J = 10$. However, due to the fact that all the transients contained in the time records to be analyzed in this section last less than a minute, we have determined that $J = 7$ gives a reasonable scale range to study the transients. In addition, a higher J would imply a shorter window of data to analyze because of the boundary effects.

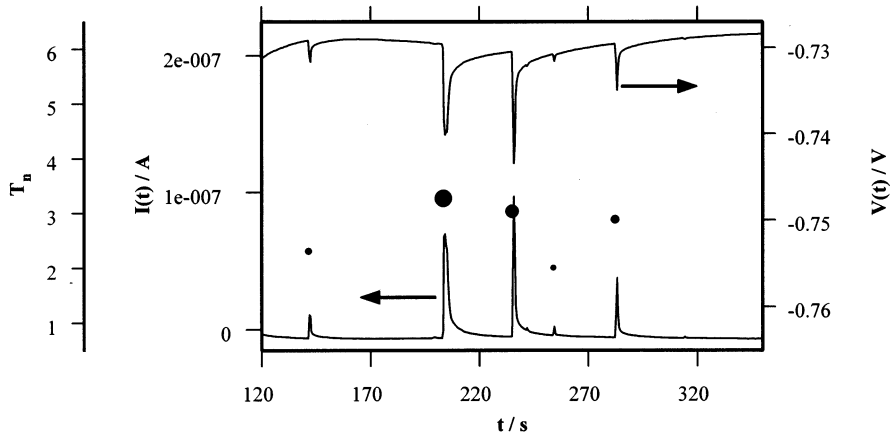

Fig. 3. Transients registered when measuring the noise from samples of AA5083 aluminum alloy after 130 h of immersion in a 0.6 M NaCl solution.

Several signals with different characteristics will be analyzed next to demonstrate the features of the algorithm.

4.1. Isolated transients with characteristic shape

The simplest case to study is the one in which the transients are so well separated from each other that a distinctive shape, characterized by a sudden increase followed by a approximately exponential decrease, can be easily distinguished. This is the case of the transients that appear in the current and potential signals plotted in Fig. 3. These time records were registered when measuring the noise from samples of AA5083 aluminum alloy after 130 h of immersion in a 0.6 M NaCl solution. These transients seem to correspond to the initiation of a deep pit, which was observed in one of the WEs at the end of this experiment.

The proposed algorithm has been applied to the time record in Fig. 3 and its result is reflected in this figure as dots. Thus, the x-position of the dots corresponds to the beginning of the detected transients, while the scale characterization T_n can be read on an additional y-axis and the relative size of the transients is reflected in the dot size. Examining Fig. 3, it can be seen that the algorithm succeeds in locating the transients although some of them are much smaller than others. In addition, the transients are characterized according to their size and scale. Thus, there are two central transients which stand out because of their greater height, while their T_n values reflect their duration.

4.2. Overlapped transients with characteristic shape

Fig. 4 shows the noise records corresponding to the same system as in Fig. 3, but 10 h later. At this time,

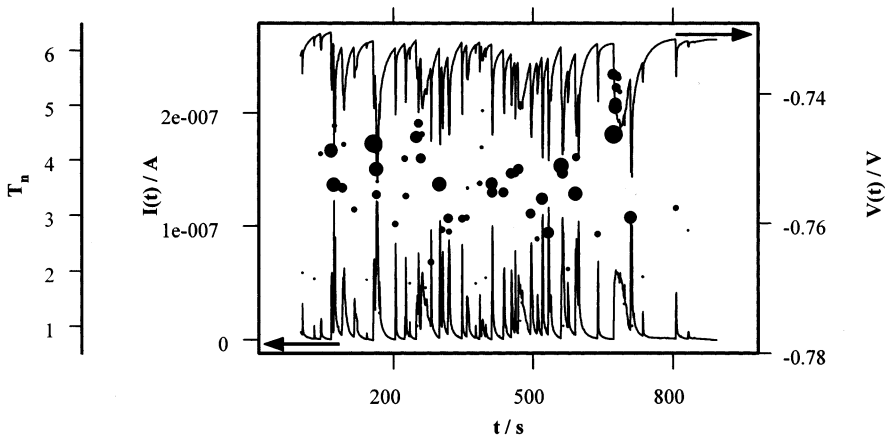

Fig. 4. Time record registered when measuring the noise from samples of AA5083 aluminum alloy after 140 h of immersion in a 0.6 M NaCl solution.

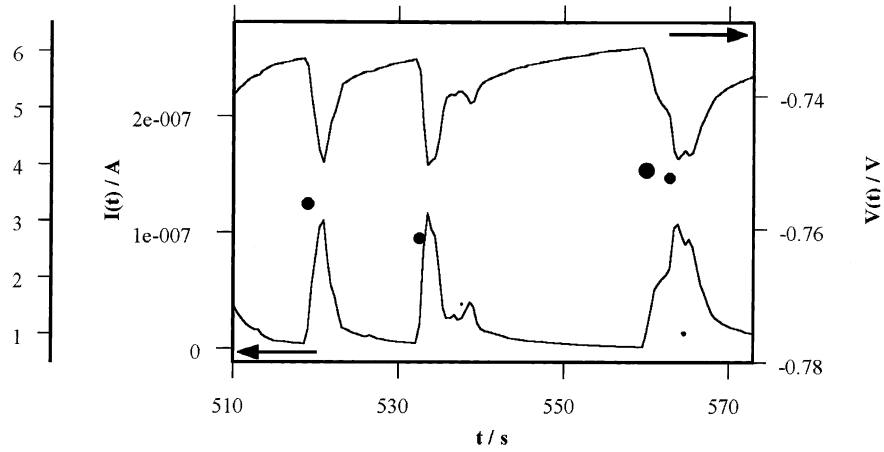

Fig. 5. Fragment of the time record in Fig. 4.

since the density of transients was much greater in this case than in the previous one, the large pit observed seems to be developing faster as a consequence of a series of micropits. Although the transients are very close, their detection is still efficient even when some transients overlap, as can be seen clearly in Fig. 5 where a portion of the time records of Fig. 4 is depicted. At first sight, it can be observed that three transients appear in the figure. However, a closer examination reveals that two of them seem to be composed of several transients that overlap. Since the algorithm was written to detect transients with a characteristic shape, those transients with anomalous shapes are considered as a superposition of transients. This feature of the algorithm is an advantage if we consider that transients with a characteristic shape have more physical meaning because their origin is the development of micropits (initiation and termination), or other localized phenomena in other cases.

4.3. Transients with odd shapes

The reliability of the algorithm decreases as the shape of the transients departs from the characteristic shape defined in Section 2.3. As an example of this, the time records plotted in Fig. 6 have been studied. These signals correspond to the noise generated by samples of type AA5083 aluminum alloy after 70 h in a 0.6 M NaCl solution doped with $CeCl_3$ at a concentration of 1.3×10^{-3} M. This register shows a transient with a characteristic shape (on the left) together with other three transients with an almost square shape. This square shape might be the consequence of a unique localized event whose intensity can be described in agreement with the shape of the transient, or else it could be considered to come from the superposition of many transients, each of which has the shape of the transient on the left of the figure. In any case, the

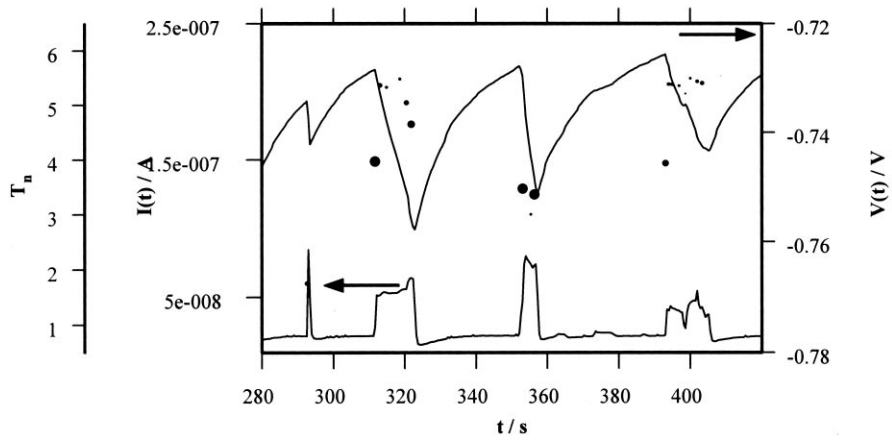

Fig. 6. Transients registered when measuring the noise from samples of AA5083 aluminum alloy after 70 h of immersion in a 0.6 M $NaCl + 1.3 \times 10^{-3}$ M $CeCl_3$ solution.

algorithm considers them as the superposition of a discrete number of transients. Unfortunately, the scale and size assigned to the transient do not match what is expected. However, the distribution of the waiting time (time elapsed between two consecutive transients) can provide valuable information about the mechanism of the process.

4.4. Changes in the voltage sign condition

Fig. 7 shows a fragment of the noise signals recorded from two AA5083 WEs which were immersed face down for 22 h in a 0.6 M NaCl solution. This time, the WEs were of square shape and had been wet-abraded down to 80 grade SiC finish. In addition, the WEs were embedded in a polyester resin without any prior coating. Such changes in the habitual experimental procedure are likely to cause the appearance of crevice corrosion, as we will see next.

In Fig. 7, several transients that are repeated almost periodically stand out. It should be noticed that the shape of the voltage transients is opposite to that shown in the time records previously depicted in this study. Thus, this time, the voltage transients show a sudden increase followed by slower decrease. The shape of this kind of transient is probably determined by a bubble evolution process, which mainly controls the cathodic reactions [11]. Apart from these sizeable transients, other smaller transients appear superposed on them. The number and shape of these smaller transients indicate that they might be the result of an anodic process occurring at the same electrode as the bubble evolution. In fact, crevice corrosion was found in one of the WEs when the samples were examined after the experiment.

If the proposed algorithm is applied using the habitual configuration, only the smaller type of transient are detected, i.e. the ones that are the consequence of an anodic process. However, the main source of noise is the group of transients caused by the bubble evolution. Hence, the opposite voltage sign condition must be imposed in the step of the algorithm explained in Section 2.2. The result of the application of the algorithm with this modification is plotted as dots in Fig. 7. This time, it has been necessary to adjust the value of X to 10 in order to get a better discrimination between the two kinds of transient. Notice that the algorithm succeeds in identifying the position of the transient. In addition, the characterization of these transients indicates that most of them are very similar in size and scale. This kind of information would enable one to detect the existence of an almost periodic process in the system, which could warn of a bubble evolution caused by a corrosion process.

5. Conclusions

An algorithm is proposed to detect and classify transients in EN records. This algorithm basically consists of two steps: a non-decimate discrete wavelet transform followed by an interscalar analysis, which should isolate transients while neglecting other components. The main advantages of the method are:

1. it is possible to establish objective criteria for defining transients;
2. this method permits the automatic and on-line detection of transients;
3. the proposed method provides information complementary to that obtained when using the customary mathematical treatments of EN.

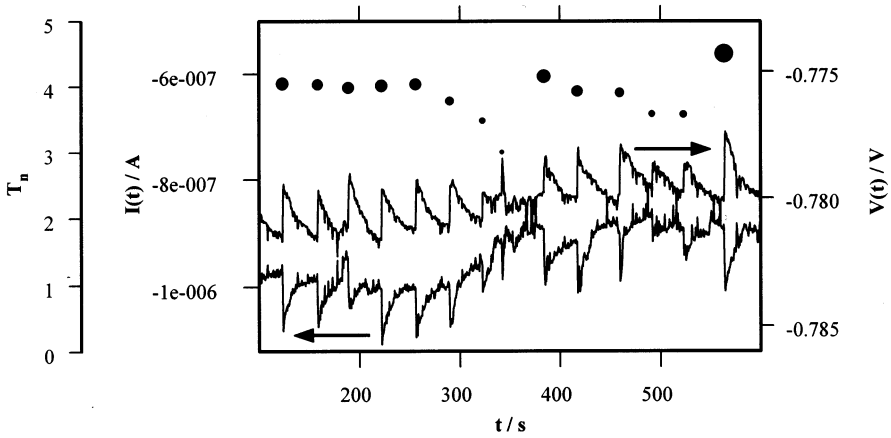

Fig. 7. Transients registered when two AA5083 WEs were undergoing crevice corrosion after 22 h placed face down in a 0.6 M NaCl solution.

The main problem of transient detection resides in defining what a transient is, since transients appear in many different shapes and sizes. However, the proposed method can be adapted to several kinds of signals. This may be achieved by choosing different wavelet bases or by changing the particular crystals to be correlated. In addition, it is necessary to set a threshold value to determine whether a correlation is sufficiently high. However, since a large gap is often found between correlated and non-correlated wavelet coefficients, the selected threshold is not decisive; this is a convenience in comparison with other methods. Hence, the best wavelet bases are those that increase such gaps. Haar wavelets have been used throughout this study because they yield the best results in the detection of transients whose initiation is very sudden.

Although further investigations are necessary to improve the proposed algorithm, it seems that an algorithm based on similar principles could become a very useful tool in the study of EN transients.

Acknowledgements

This work has received financial support from the Junta de Andalucía and the Comisión Interministerial de Ciencia y Tecnología (CICYT), projects MAT99-0625-C02-01 and 1FD97-0333-C03-02.

References

[1] P.C. Pistorius, Corrosion 53 (1997) 273.
[2] M.L. Benish, J. Sikora, B. Shaw, E. Sikora, M. Yaffe, A. Krebs, G. Martinchek, Proc. Corrosion/98, vol. 370, NACE International, Houston, 1998.
[3] J.F. Chen, W.F. Bogaerts, Corrosion 52 (1996) 753.
[4] R. Cottis, S. Turgoose, in: B.C. Syrett (Ed.), Corrosion Testing Made Easier — Electrochemical Impedance and Noise, NACE International, 1999 Ch. 7.
[5] A. Aballe, M. Bethencourt, F.J. Botana, M. Marcos, Electrochim. Acta 44 (1999) 4805.
[6] A. Aballe, M. Bethencourt, F.J. Botana, M. Marcos, Electrochem. Commun. 1 (1999) 266.
[7] A. Aballe, M. Bethencourt, F.J. Botana, M. Marcos, Rev. Metalurgia 35 (1999) 384.
[8] A. Bruce, H.-Y. Gao, Applied Wavelet Analysis with S-Plus, Springer, New York, 1996.
[9] M. Hashimoto, S. Mayajima, T. Murata, Corros. Sci. 33 (1992) 917.
[10] K.S. Anant, F.U. Dowla, Bull. Seismolog. Soc. Am. 87 (6) (1997) 1598.
[11] A. Aballe, A. Bautista, U. Bertocci, F. Huet, Proc. Corrosion/2000, vol. 424, NACE International, Houston, 2000.